Developmental exposure to polychlorinated biphenyls (PCBs) in the maternal diet causes host-microbe defects in weanling offspring mice

Kavi M Rude[1,*], **Matteo M Pusceddu**[1,*], **Ciara E Keogh**[1], **Jessica A Sladek**[1], **Gonzalo Rabasa**[1], **Elaine N Miller**[1], **Sunjay Sethi**[2], **Kimberly P Keil**[2], **Isaac N Pessah**[2], **Pamela J Lein**[2], **Mélanie G Gareau**[1,#]

[1]Department of Anatomy, Physiology and Cell Biology, School of Veterinary Medicine, University of California, Davis, Davis, CA, 95616

[2]Department of Molecular Biosciences, School of Veterinary Medicine, University of California, Davis, Davis, CA, 95616

Abstract

The gut microbiota is important for maintaining homeostasis of the host. Gut microbes represent the initial site for toxicant processing following dietary exposures to environmental contaminants. The diet is the primary route of exposure to polychlorinated biphenyls (PCBs), which are absorbed via the gut, and subsequently interfere with neurodevelopment and behavior. Developmental exposures to PCBs have been linked to increased risk of neurodevelopmental disorders (NDD), including autism spectrum disorder (ASD), which are also associated with a high prevalence of gastrointestinal (GI) distress and intestinal dysbiosis. We hypothesized that developmental PCB exposure impacts colonization of the gut microbiota, resulting in GI pathophysiology, in a genetically susceptible host. Mouse dams expressing two heritable human mutations (double mutants [DM]) that result in abnormal Ca^{2+} dynamics and produce behavioral deficits (gain of function mutation in the ryanodine receptor 1 [T4826I-*RYR1*] and a human CGG repeat expansion [170-200 CGG repeats] in the fragile X mental retardation gene 1 *[FMR1* premutation]). DM and congenic wild type (WT) controls were exposed to PCBs (0-6 mg/kg/d) in the diet starting 2 weeks before gestation and continuing through postnatal day 21 (P21). Intestinal physiology (Ussing chambers), inflammation (qPCR) and gut microbiome (16S sequencing) studies were performed in offspring mice (P28-P30). Developmental exposure to PCBs in the maternal diet caused significant mucosal barrier defects in ileum and colon (increased secretory state and tight junction permeability) of juvenile DM mice. Furthermore, PCB exposure increased the intestinal

[#]**Correspondence:** Mélanie G Gareau, School of Veterinary Medicine:APC, University of California, Davis, Davis, CA, 530-754-0605, mgareau@ucdavis.edu.
[*]These authors contributed equally

inflammatory profile (*Il6, Il1β*, and *Il22*), and resulted in dysbiosis of the gut microbiota, including altered β-diversity, in juvenile DM mice developmentally exposed to 1 mg/kg/d PCBs when compared to WT controls. Collectively, these findings demonstrate a novel interaction between PCB exposure and the gut microbiota in a genetically susceptible host that provide novel insight into environmental risk factors for neurodevelopmental disorders.

Graphical Abstract
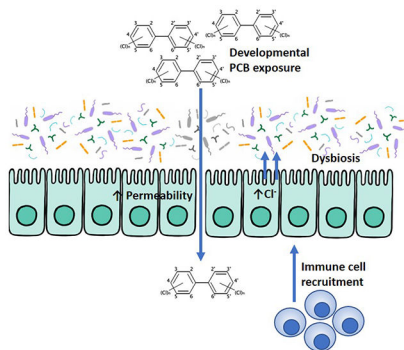
Keywords

intestinal physiology; microbiota; PCB; inflammation; neurodevelopmental disorders

INTRODUCTION

Colonization of the gastrointestinal (GI) tract with microbes begins at birth, and the composition of the microbiota is extremely plastic during early postnatal development. The neonatal period is critical for proper establishment of the microbiota, with bacterial communities undergoing dramatic changes in diversity prior to weaning (Chong et al., 2018). Compared to adults, neonates are particularly sensitive to the effects of pathological insults, such as stress (Pusceddu et al., 2015), bacterial infection (Owino et al., 2016), antibiotic treatment (Leclercq et al., 2017) or neurotoxicant exposures (Bellinger et al., 2016). This increased sensitivity is due in part to rapid development coupled with an immature gut, altered immune response, and low diversity microbiota (Belkaid and Hand, 2014; Kundu et al., 2017) during the neonatal period.

Dysbiosis induced by pathological insults during early life can have long-term impacts on the composition and diversity of the intestinal microbiota, which can have multiple downstream consequences on the physiology, immunology, and neurobiology of various organ systems, including the gut and the brain (Gareau et al., 2007). For example, in addition to diagnostic behavioral impairments, children with autism spectrum disorders (ASD) have a high risk for concurrent GI symptoms, including constipation and/or diarrhea coupled with low digestive enzyme activity, impaired intestinal barrier function, and the presence of circulating antibodies to dietary antigens (Sanctuary et al., 2018). It is widely appreciated that gene by environment interactions influence individual risk for ASD (Bolte et al., 2018); however, the mechanisms underlying these interactions remain largely

unknown. Given the strong association between behavioral impairments and GI pathophysiology, the gut microbiota may represent an exciting new link between environmental exposures, genetics, and behavioral outcomes in ASD. Therefore, studying GI physiology and the microbiota following developmental exposure to neurotoxic environmental chemicals may provide novel insights regarding the influence of environmental factors on the risk for neurodevelopmental disorders (NDD).

A ubiquitous environmental neurotoxicant of considerable interest to both gut and mental health are the class of persistent organic pollutants, known as polychlorinated biphenyls (PCBs). Early life exposures to PCBs are strongly correlated with neurological deficits in children (Berghuis et al., 2015; Grandjean and Landrigan, 2006; Sagiv et al., 2012; Schantz et al., 2003). Further, levels of PCB 95 were found to be higher in the brain of children diagnosed with a genetic form of ASD compared to neurotypical controls (Mitchell et al., 2012). Despite the ban on their production, PCBs remain prevalent in the environment, released as unintentional byproducts of contemporary industrial processes and from old buildings, equipment, and waste facilities (Fernandez-Gonzalez et al., 2011; Herrick et al., 2007; Herrick et al., 2004; Robson et al., 2010). A primary route of exposure is via the GI tract through consumption of contaminated foods (Ampleman et al., 2015; Cimenci et al., 2013); however, the impact of PCBs on the gut microbiota and potential impacts on intestinal physiology are poorly understood (Norstrom et al., 2010). Recently, PCB 126 exposure in adult mice was found to induce intestinal dysbiosis and impair host metabolism, including insulin levels, and caused increased GI and systemic inflammation as seen by elevated proinflammatory cytokines, including IFNγ (Petriello et al., 2018). Another study involving adult mice exposed to the Fox River PCB mixture found that PCBs dose-dependently impacted bile acids and this effect was mediated by the microbiota as demonstrated using germ free mice (Cheng et al., 2018). While highly novel, these studies did not assess developmental exposures, nor address the impacts of exposure on intestinal physiology.

To better understand the influence of potential interactions between genetic substrate and developmental PCB exposures on gut microbiome and function, we chose to use a mouse model of NDD that expresses two clinically relevant mutations that contribute to abnormal calcium signaling in neurons. These mutations are also of interest because they converge on the same genes/signaling pathways implicated in the developmental neurotoxicity of PCBs (Stamou et al., 2013). The first is a gain of function mutation in the ryanodine receptor (RyR) that confers susceptibility to malignant hyperthermia in humans (Dlamini et al., 2013; Pessah et al., 2010). Direct interaction of PCBs with RyR sensitize their activation to endogenous RyR modulators, and PCBs have been demonstrated to activate Ca^{2+} signaling pathways that are critical for neurodevelopment, including dendritic growth and spine formation (Lesiak et al., 2014; Wayman et al., 2012), which are known to be altered in many neurodevelopmental disorders (Stamou et al., 2013). The second genetic hit of interest is a CGG repeat expansion mutation in the fragile X mental retardation (FMR1) gene, which is the most prevalent monogenic loci associated with increased NDD risk (Krueger and Bear, 2011; Leehey and Hagerman, 2012; Willemsen et al., 2003). In mice expressing FMR1 CGG expansions <200 repeats (a model of FMR1 premutation) were shown to have chronically elevated cytoplasmic resting Ca^{2+} and μ-calpain activity in premutation neurons (Robin et

al., 2017). Co-expression of these two mutations has recently been found to confer social behavioral deficits as well as increased hippocampal dendritic arborization in juvenile mice compared to wild type congenic control mice (Keil et al., 2019).

It is becoming increasingly evident that individuals diagnosed with NDDs, like ASD, display altered gut microbiome compositions compared to typically developing individuals (De Angelis et al., 2013; Kang et al., 2018). Yet whether this dysbiosis is caused by genetic or environmental stimuli, or both, remains unknown. Using a mixture of PCBs based on the congener profile found in pregnant women at increased risk of having a child with a NDD (Barkoski et al., 2018; Sethi et al., 2019), we asked whether developmental exposure to PCBs impacts colonization of the gut microbiota, intestinal permeability, and the mucosal immune response. Finally, we hypothesized that mice that express heritable mutations that contribute to abnormal neuronal Ca^{2+} dynamics and are associated with neurobehavioral impairments would be more susceptible to PCB-induced gut effects than WT congenic mice.

MATERIALS AND METHODS

Mice

This study utilized mice expressing a human gain-of-function mutation in RyR1 (T4826I-*RYR1*) and a human CGG repeat expansion (170-200 CGG repeats) in the FMR1 gene (premutation range), which are referred to as the double mutant [DM] mice, or congenic wildtype (WT: 75% C57BL/6; 25% Sv129 as determined by SNP analysis) mice. The DM mouse was previously described (Keil et al., 2019). CGG repeat lengths were confirmed using Expanded High Fidelity Plus PCR System (Roche Diagnostics, Indianapolis, IN) as described previously (Chen et al., 2010). Genotyping of T4826I was confirmed as described previously (Barrientos et al., 2012). Briefly the PCR conditions for the mutant reaction consisted of 0.5 μM of forward and reverse mutant primers, 1x GoTaq buffer, 2 mM MgCl2, 0.4 mM dNTP and 0.25 μl GoTaq Polymerase. The reaction for the WT gene consisted of 0.53 μM forward wild type primer, 0.57 μM reverse wild type primer, 1x GoTaq buffer, 2 mM MgCl2, 0.4 mM dNTP, 0.25 μl GoTaq Polymerase. PCR conditions were as follows. Mutant; 95°C for 3 min, 40 cycles of 95°C for 30 sec, 60°C for 30 sec, 72°C for 30 sec and a final extension of 72°C for 10 min. WT: 95°C for 3 min, 40 cycles of 95°C for 30 sec, 55°C for 30 sec, 72°C for 30 se c and a final extension of 72°C for 10 min. PCR product was run on a 1.5% agarose gel at 125 V for 30 min; the expected size of mutant band was 100 bp, and WT, 353 bp.

Mice were bred in-house in a specific pathogen-free vivarium and kept in clear plastic cages containing corn cob bedding and maintained on a 12 h light and dark cycle at $22 \pm 2°C$. Food (Diet 5058, LabDiet, Saint Louis, MO) and water were available *ad libitum.* Mice were euthanized by CO_2 asphyxiation followed by cervical dislocation. All procedures involving animals were conducted in accordance with the NIH Guide for the Care and Use of Laboratory Animals and were approved by the University of California Davis Animal Care and Use Committee (IACUC #20584).

PCBs

The MARBLES (Markers of Autism Risk in Babies – Learning Early Signs) (Hertz-Picciotto et al., 2018) PCB mixture corresponds to the relative proportion of the 12 most abundant PCBs measured in serum from mothers at elevated risk for having a child with a NDD in a UC Davis MIND institute study (Sethi et al., 2019). PCBs for this study were synthesized by Dr. Hans Joachim Lehmler (University of Iowa, Iowa City, IA) and were > 99% pure as determined by ^{1}H-NMR, ^{13}C-NMR, and GC-MS, as previously described (Sethi et al., 2019). The MARBLES mix includes the following PCBs listed by descending proportion (%): PCB 28 (48.2), PCB 11 (24.3), PCB 118 (4.9), PCB 101 (4.5), PCB 153 (3.1), PCB 180 (2.8), PCB 149 (2.1), PCB 138 (1.7), PCB 84 (1.5), PCB 135 (1.3) and PCB 95 (1.2). The MARBLES mix was dissolved in organic peanut oil (Spectrum Organic Products, LLC, Melville, NY) and provided to dams daily via organic peanut butter (Trader Joe's, Monrovia, CA).

Study Design

The experimental design is schematized in Figure 1. Adult primiparous female mice were randomly assigned to a PCB dose group at the beginning of the study. Vehicle or the PCB mixture (0.1, 1, or 6mg/kg/day; 8 litters per treatment) was administered daily in the dam's home cage beginning two weeks prior to mating and continued until weaning at postnatal day 21 (P21). Tissues were collected from juvenile male and female mice at P28-P30 for assessment of intestinal function, inflammation, and microbiota analysis. One male and one female mouse per litter were used per experiment to avoid litter effects. No sex effects were observed; therefore, all data are presented as combined males and females of equal proportion.

Ussing chambers

Ussing chamber studies were performed to assess intestinal physiology (Clarke, 2009). Briefly, a small piece of intestinal tissue (distal ileum and proximal colon) was collected from individual animals, cut along the mesenteric border, and mounted on Ussing chambers (Physiological Instruments, San Diego, CA), exposing 0.1 cm^2 of tissue area to circulating oxygenated Ringer's buffer maintained at 37°C. The Ringer's buffer was made of (in mM): 115 NaCl, 1.25 CaCl$_2$, 1.2 MgCl$_2$, 2.0 KH$_2$PO$_4$ and 25 NaHCO$_3$ at pH 7.35 ± 0.02. Glucose (10 mM) was added to the serosal compartment as a source of energy, which was osmotically balanced with mannitol (10 mM) in the mucosal compartment. Ion transport and permeability across the tissue layer were assessed in real time. Active ion transport was measured by short-circuit current (Isc) at baseline, along with conductance (G) as a marker of paracellular, tight junction permeability. Macromolecular permeability was assessed by mucosal to serosal flux of FITC-labeled dextran (Sigma; 4 kDa), which was measured by sampling every 30 min on the serosal side.

Histology

Ileal and colonic tissue segments were collected and drop fixed in 10% neutral buffered formalin for 48h then transferred to 70% isopropyl alcohol for dehydration and processed for paraffin embedding. Paraffin blocks were cut using a microtome (4 um sections) onto

glass slides and processed for hematoxylin and eosin (H&E) staining. Briefly, slides were de-paraffinized and re-hydrated followed by staining and subsequent dehydration. Tissue was then cleared in histoclear and mounted with xylene based permount mounting media. Images were taken at 20X on a Nikon Eclipse E600 microscope using a Nikon Digital Sight DS-U3 camera to assess for damage and representative images are presented.

qPCR

Gene expression by qPCR analysis was performed on colonic and ileal tissue samples. Tissue was collected and stored in Trizol, and RNA was extracted as per the manufacturer's instructions (Life Technologies). mRNA was transcribed into cDNA (Bio-Rad, iScript) and amplified using SYBR green (Life Technologies). Pro-inflammatory cytokines, including interleukin *(Il)6, Il12,* and *Il1β* and the regulatory cytokine *Il22* were quantified. In addition, pattern recognition receptors (PRR) important in innate immunity, including nucleotide oligomerization domain *(Nod)1* and *Nod2,* were quantified as was the anti-microbial peptide *RegIIIγ*. Primers were obtained from Primerbank and validated by standard curve (Table 1).

Microbiota analysis

Frozen fecal samples collected at euthanasia were processed by the UC Davis mouse metabolic phenotyping core (MMPC; NIH funded) and Host Microbe Systems Biology Core (HMSBC). Total bacterial DNA was extracted using the Mo-Bio (now Qiagen) PowerFecal kit. Sample libraries were prepared and analyzed by bar coded amplicon sequencing. In brief, the purified DNA was amplified on the V4 region of the 16S rRNA genes via PCR using the following primers: F319 (5'-ACTCCTACGGGAGGCAGCAGT-3') and R806 (5'-GGACTACNVGGGTWTCTAAT-3'). High-throughput sequencing was performed with Illumina MiSeq paired end 250-bp run. Sequencing was performed by the UC Davis HSMBC and analysis by the MMPC. Raw sequences have been uploaded to the SRA (Sequence Read Archive) under accession SRP151673.

The data derived from sequencing was processed using QIIME2 for 16S based microbiota analyses (QIIME 2 Development Team (2017)). Demultiplexed paired end sequences that already had barcodes and adapters removed were analyzed using QIIME2 version 2017.12.1. For quality filtering and feature operational taxonomic unit (OTU) prediction, we used DADA2 (Callahan et al., 2016). Upon reviewing the sequence quality data, we trimmed 0 nucleotides from the 5' end of the forward and 0 nucleotides from the reverse reads. Forward reads were truncated to 270 nucleotides and reverse reads to 220 nucleotides. Representative sequences were aligned using MAFFT (Katoh and Standley, 2013). A phylogenetic tree of the aligned sequences was made using FastTree 2 (Price et al., 2010). OTUs/features were taxonomically classified using a pre-trained Naive Bayes taxonomy classifier. The classifier was trained using the Silva 128 97% OTUs for the 319F-806R region (Quast et al., 2013). Tables of taxonomic counts and percentage (relative frequency) were generated. Diversity analyses were run on the resulting OTU/feature.biom tables to provide both phylogenetic and non-phylogenetic metrics of alpha and beta diversity (Lozupone et al., 2011). Additional data analysis, including the partial least squares - discriminant analysis (PLS-DA) and statistics were performed with R.

Statistics

Data in all figures are presented as the mean ± SEM. Statistical significance was determined using the Student's T-test or ANOVAs as appropriate followed by post-hoc analysis using the Tukey's test as indicated. Data was tested for normality and parametric versus non-parametric analyses were performed as appropriate. All analyses were performed using GraphPad Prism (San Diego, CA) and p values less than 0.05 were deemed significant.

RESULTS

Developmental PCB exposure increased gut permeability in juvenile DM mice in a dose-dependent manner.

Since dietary consumption is a significant route of exposure to PCBs, GI physiology was characterized in juvenile mice following gestational and neonatal exposures via the maternal diet. Small (ileum) and large (colon) bowel physiology was assessed for secretory state (Isc), paracellular (G), and macromolecular (FITC-dextran flux) permeability using an Ussing chamber system. In the colon, there was no influence of genotype on baseline Isc in the absence of PCB exposure (Figure 2A). Baseline Isc was significantly increased in DM mice exposed to 1, but not 0.1 or 6 mg/kg/d PCBs in the maternal diet (Figure 2A). Similarly, tight junction permeability, as determined by measurement of conductance (G), was not influenced by genotype in the absence of developmental PCB exposure but was significantly increased in DM mice compared to WT mice exposed to PCBs at 1 but not 0.1 or 6 mg/kg/d in the maternal diet (Figure 2B). Consistent with these findings, macromolecular permeability, as indicated by increased mucosal to serosal transit of 4 KDa FITC-labeled dextran, was increased at 0-30, 30-60 and 90-120 minutes in the 1 mg/kg/d DM mice versus 1 mg/kg/d WT group (Figure 2C) but not significantly altered from WT control animals in the other experimental groups. Histology did not reveal the presence of any overt damage in either group compared to WT controls as determined using the Wallace score (Reardon et al., 2011) (Figure 2D).

In the ileum, genotype influenced baseline Isc, causing a significant increase in DM relative to WT mice (Figure 3A). Developmental PCB exposure significantly increased baseline Isc in WT mice in the 0.1 mg/kg/d dose group; however, no impact of PCB dose on Isc was observed in DM mice (Figure 3A). In contrast, genotype and PCB effects on conductance in the ileum were similar to observations in the colon. Conductance (G) was significantly increased only in DM mice in the 1 mg/kg/d PCB dose group (Figure 3B), with no impact of PCB exposure seen in WT mice. Macromolecular permeability (FITC-dextran flux; Figure 3C) showed a significant increase in DM mice following 6 mg/kg/d PCB exposure compared to genotype-matched vehicle controls; and a significant increase in permeability was also observed between WT and DM mice exposed to PCBs at 1 mg/kg/d but not at the other exposure doses (Figure 3C). Similar to the colon, histological analysis did not reveal any evidence of overt damage in either group (Figure 3D).

Developmental PCB exposure altered cytokines levels and markers of immune protection in both DM and WT juvenile mice.

Mucosal immunity was assessed by qPCR in both the colon and ileum from juvenile WT and DM mice following developmental exposure to vehicle or PCBs at 1 mg/kg/d in the maternal diet. In the colon, developmental PCB exposure increased *Il6, Il1β* and *Il22* mRNA expression levels in both WT and DM mice compared to genotype-matched vehicle controls with no change in *Il12* expression (Figure 4A). *RegIIIγ*, an antimicrobial lectin, was increased in DM mice following PCB exposure (1 mg/kg/d). Finally, no differences between groups were found in the expression of the bacterial PRRs *Nod1* and *Nod2* (Figure 4A).

In the ileum, genotype alone more strongly influenced mucosal immunity, in contrast to the colon. *Il6* expression was increased in WT mice exposed to PCB, similarly to that seen in the colon. In DM mice, exposure to 1 mg/kg/d PCBs increased the expression of *Il6, Il12,* and *Il22* compared to vehicle DM controls (Figure 4B). In contrast to colonic tissues, *Nod1* and *Nod2* expression were increased in the ileum of DM mice at both 0 and 1mg/kg/d exposure to PCBs, with the exception of basal *Nod1* levels which were decreased compared to WT mice (Figure 4B). Finally, Il12 and *RegIIIγ* were increased in DM mice vs WT mice exposed to 1 mg/kg/d PCBs indicating the presence of a genotype plus exposure effect.

Developmental exposure to PCBs altered the composition of the microbiota in DM mice versus WT controls.

To determine whether developmental PCB exposure alters the composition of the fecal microbiota in offspring, we used an unbiased approach with 16S Illumina sequencing. Fecal samples collected from juvenile mice developmentally exposed to PCBs via the maternal diet revealed that a combination of genetic and environmental factors impact the composition of the fecal microbiota. Beta diversity was measured using the Bray-Curtis method, followed by statistical analysis using permutational multivariate analysis of variance (PERMANOVA), and subsequently analysis of similarities (ANOSIM) and pairwise comparisons of group mean dispersions (PERMDISP) (Paliy and Shankar, 2016). PERMANOVA (Anderson, 2008) and ANOSIM (Clarke, 1993) revealed statistical difference between vehicle treated WT vs DM mice (Figure 5A; Table 2). In contrast, no difference was seen using PERMDISP. Exposure to 1 mg/Kg/d PCB led to a greater difference in beta diversity, as demonstrated by significance seen by all three analysis methods (Figure 6A; Table 2). Given the weaker factor effect, identified by lower pseudo-F (PERMANOVA), and R values (ANOSIM), as well as no significant group dispersion (PERMDISP) found in the vehicle WT vs DM comparison (Table 2), this suggests that exposure to 1 mg/kg/d of PCBs further exacerbated the difference in beta diversity between the microbiota in WT and DM mice (Figure 5A–6A).

Linear discriminant analysis effect size (LefSe) was used to identify the most differentially abundant taxa between vehicle treated WT and DM mice (Figure 5B) and mice developmentally exposed to PCBs at 1 mg/kg/d in the maternal diet (Figure 6B). A greater abundance in the Deferribacteres and Proteobacteria phyla, including the Epsilonproteobacteria class were identified in vehicle-treated DM mice compared to the WT mice (Figure 5B). Similarly, a greater abundance of taxa within the Proteobacteria phyla,

specifically within the Deltaproteobacteria and Betaproteobacteria class, and a greater abundance in the Deferribacteres phyla was identified in DM mice compared to the WT mice following exposure to 1 mg/kg/d PCB dose group (Figure 6B). The cladogram depicts phylum, class, order, family, and genus going from inner to outer rings (left panel) with effect size represented by the linear discriminate analysis (LDA; right panel) score plot. Overall, the phylum level abundance also identified a lower percentage of Bacteroidetes levels in DM mice exposed to either vehicle or 1 mg/kg/d PCBs compared to their respective exposure-matched WT controls (Figure 7). Proteobacteria levels were increased in DM vehicle control mice relative to WT vehicle control mice, and in both WT and DM mice exposed to 1 mg/kg/d PCBs relative to their genotype-matched vehicle controls (Figure 7).

At the genus level, developmental exposure to PCBs at 1 mg/kg/d in the maternal diet reduced the abundance of Bacteroidales S7-24 in both WT and DM mice (Figure 8A). In contrast, there was an increase in relative abundance of Lactobacillus (Figure 8B) and Lachnospiraceae (Figure 8C) in DM mice, both in vehicle and following exposure to 1mg/Kg/d, compared to WT controls. Finally, abundance of Alistipes was decreased in WT mice following exposure to 1 mg/kg/d of PCBs and in DM vehicle controls compared to WT vehicle controls (Figure 8C).

DISCUSSION

Detrimental impacts on GI physiology in response to environmental toxin exposures are frequently overlooked, even though the diet is a significant route of exposure. Since the development of the GI tract coincides with neural development (Borre et al., 2014), and changes in GI physiology have been shown to alter neurodevelopmental outcomes (Bruce-Keller et al., 2014), studying GI physiology following exposures to neurodevelopmental toxicants is timely. Determining whether developmental exposure to PCBs modulates the composition of the microbiota in offspring and whether this is impacted by genetic predisposition to NDDs could yield important insight into mechanisms by which environmental factors interact with genetic susceptibilities to influence NDD risk. Recent evidence points to PCB exposure in adult mice detrimentally impacting the gut microbiota, with decreased diversity demonstrated as measured by the Shannon diversity index (Chi et al., 2018). A combination of dioxin-like (PCB 77 and 126) and non-dioxin like (PCB153) PCBs administered to adult mice weekly for 6 weeks impacted the microbiota following feeding of a high-fat diet (Chi et al., 2018). Similarly, PCB 126 exposure to adult mice caused reductions in alpha diversity coupled with decreases in levels of the beneficial genera Bifidobacteria and Lactobacillus (Petriello et al., 2018). Here we establish that developmental exposure to an environmentally relevant mixture of PCBs via the maternal diet results in intestinal dysbiosis and altered GI physiology in juvenile offspring that are genetically susceptible to neurobehavioral impairments (Keil et al., 2019). Together, these data demonstrate that in a mouse model expressing multiple mutations shown to produce abnormal Ca^{2+} dynamics in neurons, also exhibits GI pathophysiology and dysbiosis of the GI microbiome, which is further impaired following developmental PCB exposure.

The GI tract has numerous mechanisms in place to protect it against various noxious insults, including production of anti-microbial peptides, mucus release, and maintenance of a tight

epithelial barrier by modulation of tight junction and scaffolding proteins (Sharkey et al., 2018). The commensal microbiota that reside within the outer mucus layer also play a protective role in limiting access of potentially pathogenic organisms to the host epithelium (Johansson et al., 2015). Therefore, exposures to environmental toxicants that impact the composition of the microbiota could potentially create a more vulnerable host via detrimentally impacting one or more of these protective barriers. Should these environmental exposures occur either during development or early neonatal life when many of these protective GI mechanisms are still developing, this can have long-lasting adverse consequences for the host. Previous studies looking at GI physiology following oral administration of a single bolus of PCBs to adult mice identified GI permeability deficits as determined by increased serum FITC-labeled dextran levels (Choi et al., 2010). However, a role for environmental neurotoxicants, including PCBs, in modulating the developing gut remains unknown. In our current study, we identified pathophysiology of both the colon and ileum in mice developmentally exposed to PCBs, which co-express two mutations in genes implicated in NDDs. In juvenile mice (P28-30), developmental exposure to PCBs led to an increased secretory state, increased tight junction permeability, and increased macromolecular permeability in the genetically susceptible host that was not observed in similarly exposed WT mice. This exposure was dose-dependent, with the 1 but not 0.1 or 6 mg/kg/d PCB dose significantly affecting colonic and intestinal physiology. While the physiological reasons for this particular absence of response in intestinal physiology seen at the higher 6 mg/kg/d dose remain unknown, similar non-monotonic dose-response relationships have been previously reported for effects of developmental PCB exposure on neurodevelopmental outcomes (Wayman et al., 2012; Yang et al., 2009). These findings suggest that in a genetically susceptible host, developmental PCB exposures lead to a more secretory and permeable GI tract, which would make the host more vulnerable to exposure to noxious antigens or pathogens, allowing increased systemic uptake. Patients with ASD have been demonstrated to have increased levels of serum zonulin, which regulates epithelial cell tight junction proteins and has been used as a surrogate marker for intestinal permeability (Esnafoglu et al., 2017). Intestinal tissue samples from ASD patients were also found to have decreased barrier forming tight junction proteins and increased pore forming proteins supporting the presence of increased permeability (Fiorentino et al., 2016). Altered intestinal barrier function, coupled with a leakier blood brain barrier and the presence of neuroinflammation (Fiorentino et al., 2016) suggests pathologic uptake of luminal antigens causing downstream effects negatively impacting the CNS.

The mucosal immune response in the gut is critical for regulating host-microbe interactions and preventing overt immune responses to innocuous bacterial organisms (Sharkey et al., 2018). The GI epithelium is in close contact to a wide array of innate and adaptive immune cells within the underlying lamina propria, which can respond to threats that breach the protective mechanisms of the epithelial barrier (Sharkey et al., 2018). In this study, distinct patterns of inflammatory responses were seen in the ileum and colon with pro-inflammatory cytokines indicative of the presence of mild inflammation in both the small and large intestine in DM mice and this effect of genotype was slightly compounded by PCB exposure. Similarly, the PRRs Nod1 and Nod2 that bind to bacterial peptidoglycan to induce an NF-κB dependent innate immune response (Mukherjee et al., 2018), were only impacted

in the ileum but not the colon in DM mice at baseline, with exposure to PCBs compounding this effect. In contrast, the antimicrobial peptide *RegIIIγ* demonstrated similar effects in both the colon and ileum of DM mice, with increases in expression levels seen following PCB exposure. Recent studies have determined that region-specific differences exist in the microbiota composition and subsequent proteome analysis, which could contribute to changes in host responses (Lichtman et al., 2016). Given the change observed in *RegIIIγ* expression, alterations in mucosa-associated bacteria would be of interest for future studies. Overall, these findings suggest that while PCBs can impact the gut immune response, this effect is enhanced in a genetically susceptible host.

Ryanodine receptors are expressed in the GI tract and are associated with pace-making functions of the interstitial cells of Cajal (ICC) by regulating release of intracellular calcium (Baker et al., 2016; Zhu et al., 2015). ICC express multiple RyRs, with RyR2 being predominant, which work together with inositol triphosphate receptors to mediate Ca^{2+} release (Baker et al., 2016). ICCs are important in coordinating propulsion along the gut, with impairments in pace-making causing constipation or diarrhea. Non-CNS pathology, including the GI tract, have also been seen in fragile-X premutation carriers and in CGG knock-in mice, with neuronal inclusions identified in enteric nerves (Hunsaker et al., 2011). Taken together, these studies suggest that predisposition to altered intestinal physiology in our DM mice may result from altered ENS signaling, which triggers pathophysiology following PCB exposure and subsequent dysbiosis. The precise cellular mechanisms involved within the GI tract that result in altered host-microbe interactions and subsequent pathophysiology remain to be determined.

The gut microbiota is increasingly being associated with playing a critical role in maintaining overall health and well-being, with dysbiosis seen in numerous disease states, including many outside of the GI tract, such as ASD (Rose et al., 2018), depression (Mayer et al., 2014), diabetes (Knip and Siljander, 2016; Larsen et al., 2010), and multiple sclerosis (Bhargava and Mowry, 2014). PCB exposure was previously found to alter the composition and structure of the microbiota, with oral exposure of PCBs to adult mice decreasing the levels of proteobacteria, which could be attenuated by beneficial behavioral factors such as voluntary exercise (Choi et al., 2013). Despite these findings, it remains unknown whether environmental neurotoxicant exposure during development leads to long-lasting dysbiosis. In the current study, DM mice displayed differences in microbial abundances when compared to WT vehicle-treated control mice, which were more pronounced following exposure to PCBs. Moreover, an increase in abundance of bacterial species reported to be associated with a state of inflammation was found at the phylum level (Rizzatti et al., 2017). This was further enhanced by developmental exposure to PCBs, resulting in a microbiota populated by some communities associated with increased inflammation, such as Proteobacteria. This dysbiosis was accompanied by an increased secretory state and increased permeability of the gut, which, coupled with the altered mucosal immune response, would enhance the ability of neurotoxicants to cross the epithelium, and subsequently increase their distribution throughout the body. While our study cannot directly decipher whether the dysbiosis led to changes in gut physiology or vice-versa, based on the existing literature (Cheng et al., 2018; Chi et al., 2018; Petriello et al., 2018), it would be suspected that the PCBs could directly interact with gut microbes, leading to a shift in the

composition of the microbiota, and a subsequent decrease in intestinal barrier function, which would allow systemic entry of the PCBs in a genetically susceptible host.

The prevalence of NDDs, including ASD, attention deficit/hyperactivity disorder (ADHD) and obsessive-compulsive disorders have been increasing in recent years with no clear etiology (Antshel and Russo, 2019). These NDDs are increasingly being associated with the presence of co-morbid GI symptoms and intestinal dysbiosis (Dinan and Cryan, 2017). Highlighting this observation, the presence of a maternal microbiota that is skewed towards induction of a T helper17-like immune response increases the likelihood of development of NDDs in offspring in a mouse model of ASD involving maternal immune activation (MIA) (Kim et al., 2017). Furthermore, the GI tract is increasingly appreciated as a critical site of uptake of numerous environmental neurotoxicants, including PCBs, which are plausible risk factors for NDDs (Cheslack-Postava et al., 2013; Lyall et al., 2017; Sagiv et al., 2010). Given that the gut is colonized by trillions of commensal microbes, and these microbes are critical in maintaining host-microbe interactions, exposure to environmental neurotoxicants via the gut has the potential to negatively impact these interactions. The gut and brain communicate bi-directionally via the MGB axis (Dinan and Cryan, 2017; Pusceddu et al., 2018), therefore, altered host-microbe interactions may serve as a novel mechanism through which PCBs mediate their detrimental effects on the brain and potentially lead to the development of NDDs.

In conclusion, our findings support a role for the GI tract as a primary target site of PCB exposure, which can detrimentally impact GI physiology and lead to changes in the composition of the gut microbiota, and alter the mucosal immune response, with this effect significantly enhanced in mice expressing NDD susceptibility genes. This study identifies a novel mechanism of PCB developmental toxicity that may have long-term health consequences on not only GI, but also neural function. These studies also describe a novel model for studying mechanisms by which PCBs interact with genetic susceptibility factors to influence individual risk for NDDs, and they identify the gut microbiome as a novel therapeutic target for reducing the effects of developmental PCB exposure on human health.

ACKNOWLEDGMENTS

Abbreviations

ASD	autism spectrum disorder
FMR1	fragile X mental retardation
G	conductance

GI	gastrointestinal
IBD	inflammatory bowel disease
Isc	short circuit current
MARBLES	markers of autism risk in babies - learning early signs
MGB axis	microbiota-gut-brain axis
NDD	neurodevelopmental disorders
PCB	polychlorinated biphenyls
Ryr1	ryanodine receptor 1

REFERENCES

Ampleman MD, Martinez A, DeWall J, Rawn DF, Hornbuckle KC, Thorne PS, 2015 Inhalation and dietary exposure to PCBs in urban and rural cohorts via congener-specific measurements. Environ Sci Technol 49, 1156–1164. [PubMed: 25510359]

Anderson MJ, 2008 A new method for non-parametric multivariate analysis of variance. Austral Ecology 26.

Antshel KM, Russo N, 2019 Autism Spectrum Disorders and ADHD: Overlapping Phenomenology, Diagnostic Issues, and Treatment Considerations. Curr Psychiatry Rep 21, 34. [PubMed: 30903299]

Baker SA, Drumm BT, Saur D, Hennig GW, Ward SM, Sanders KM, 2016 Spontaneous Ca(2+) transients in interstitial cells of Cajal located within the deep muscular plexus of the murine small intestine. J Physiol 594, 3317–3338. [PubMed: 26824875]

Barkoski J, Bennett D, Tancredi D, Barr DB, Elms W, Hertz-Picciotto I, 2018 Variability of urinary pesticide metabolite concentrations during pregnancy in the MARBLES Study. Environ Res 165, 400–409. [PubMed: 29860212]

Barrientos GC, Feng W, Truong K, Matthaei KI, Yang T, Allen PD, Lopez JR, Pessah IN, 2012 Gene dose influences cellular and calcium channel dysregulation in heterozygous and homozygous T4826I-RYR1 malignant hyperthermia-susceptible muscle. J Biol Chem 287, 2863–2876. [PubMed: 22139840]

Belkaid Y, Hand TW, 2014 Role of the microbiota in immunity and inflammation. Cell 157, 121–141. [PubMed: 24679531]

Bellinger DC, Matthews-Bellinger JA, Kordas K, 2016 A developmental perspective on early-life exposure to neurotoxicants. Environ Int 94, 103–112. [PubMed: 27235688]

Berghuis SA, Bos AF, Sauer PJ, Roze E, 2015 Developmental neurotoxicity of persistent organic pollutants: an update on childhood outcome. Arch Toxicol 89, 687–709. [PubMed: 25618547]

Bhargava P, Mowry EM, 2014 Gut microbiome and multiple sclerosis. Curr Neurol Neurosci Rep 14, 492. [PubMed: 25204849]

Bolte S, Girdler S, Marschik PB, 2018 The contribution of environmental exposure to the etiology of autism spectrum disorder. Cell Mol Life Sci.

Borre YE, O'Keeffe GW, Clarke G, Stanton C, Dinan TG, Cryan JF, 2014 Microbiota and neurodevelopmental windows: implications for brain disorders. Trends Mol Med 20, 509–518. [PubMed: 24956966]

Bruce-Keller AJ, Salbaum JM, Luo M, Blanchard E.t., Taylor CM, Welsh DA, Berthoud H R., 2014 Obese-type Gut Microbiota Induce Neurobehavioral Changes in the Absence of Obesity. Biol Psychiatry.

Callahan BJ, McMurdie PJ, Rosen MJ, Han AW, Johnson AJ, Holmes SP, 2016 DADA2: High-resolution sample inference from Illumina amplicon data. Nat Methods 13, 581–583. [PubMed: 27214047]

Chen Y, Tassone F, Berman RF, Hagerman PJ, Hagerman RJ, Willemsen R, Pessah IN., 2010 Murine hippocampal neurons expressing Fmr1 gene premutations show early developmental deficits and late degeneration. Hum Mol Genet 19, 196–208. [PubMed: 19846466]

Cheng SL, Li X, Lehmler HJ, Phillips B, Shen D, Cui JY, 2018 Gut Microbiota Modulates Interactions Between Polychlorinated Biphenyls and Bile Acid Homeostasis. Toxicol Sci 166, 269–287. [PubMed: 30496569]

Cheslack-Postava K, Rantakokko PV, Hinkka-Yli-Salomaki S, Surcel HM, McKeague IW, Kiviranta HA, Sourander A, Brown AS, 2013 Maternal serum persistent organic pollutants in the Finnish Prenatal Study of Autism: A pilot study. Neurotoxicol Teratol 38, 1–5. [PubMed: 23591055]

Chi Y, Lin Y, Zhu H, Huang Q, Ye G, Dong S, 2018 PCBs-high-fat diet interactions as mediators of gut microbiota dysbiosis and abdominal fat accumulation in female mice. Environ Pollut 239, 332–341. [PubMed: 29674211]

Choi JJ, Eum SY, Rampersaud E, Daunert S, Abreu MT, Toborek M, 2013 Exercise attenuates PCB-induced changes in the mouse gut microbiome. Environ Health Perspect 121, 725–730. [PubMed: 23632211]

Choi YJ, Seelbach MJ, Pu H, Eum SY, Chen L, Zhang B, Hennig B, Toborek M, 2010 Polychlorinated biphenyls disrupt intestinal integrity via NADPH oxidase-induced alterations of tight junction protein expression. Environ Health Perspect 118, 976–981. [PubMed: 20299304]

Chong CYL, Bloomfield FH, O'Sullivan JM, 2018 Factors Affecting Gastrointestinal Microbiome Development in Neonates. Nutrients 10.

Cimenci O, Vandevijvere S, Goscinny S, Van Den Bergh MA, Hanot V, Vinkx C, Bolle F, Van Loco J, 2013 Dietary exposure of the Belgian adult population to non-dioxin-like PCBs. Food Chem Toxicol 59, 670–679. [PubMed: 23811102]

Clarke KR, 1993 Non-parametric multivariate analyses of changes in community structure. Australian Journal of Ecology 18.

Clarke LL, 2009 A guide to Ussing chamber studies of mouse intestine. Am J Physiol Gastrointest Liver Physiol 296, G1151–1166. [PubMed: 19342508]

De Angelis M, Piccolo M, Vannini L, Siragusa S, De Giacomo A, Serrazzanetti DI, Cristofori F, Guerzoni ME, Gobbetti M, Francavilla R, 2013 Fecal microbiota and metabolome of children with autism and pervasive developmental disorder not otherwise specified. PLoS One 8, e76993. [PubMed: 24130822]

Dinan TG, Cryan JF, 2017 The Microbiome-Gut-Brain Axis in Health and Disease. Gastroenterol Clin North Am 46, 77–89. [PubMed: 28164854]

Dlamini N, Voermans NC, Lillis S, Stewart K, Kamsteeg EJ, Drost G, Quinlivan R, Snoeck M, Norwood F, Radunovic A, Straub V, Roberts M, Vrancken AF, van der Pol WL, de Coo RI, Manzur AY, Yau S, Abbs S, King A, Lammens M, Hopkins PM, Mohammed S, Treves S, Muntoni F, Wraige E, Davis MR, van Engelen B, Jungbluth H, 2013 Mutations in RYR1 are a common cause of exertional myalgia and rhabdomyolysis. Neuromuscul Disord 23, 540–548. [PubMed: 23628358]

Esnafoglu E, Cirrik S, Ayyildiz SN, Erdil A, Erturk EY, Dagli A, Noyan T, 2017 Increased Serum Zonulin Levels as an Intestinal Permeability Marker in Autistic Subjects. J Pediatr 188, 240–244. [PubMed: 28502607]

Fernandez-Gonzalez R, Martinez-Carballo E, Gonzalez-Barreiro C, Rial-Otero R, Simal-Gandara J, 2011 Distribution of polychlorinated biphenyls in both products and by-products of a mussel shell incinerator facility. Environ Sci Pollut Res Int 18, 1139–1146. [PubMed: 21336633]

Fiorentino M, Sapone A, Senger S, Camhi SS, Kadzielski SM, Buie TM, Kelly DL, Cascella N, Fasano A, 2016 Blood-brain barrier and intestinal epithelial barrier alterations in autism spectrum disorders. Mol Autism 7, 49. [PubMed: 27957319]

Gareau MG, Jury J, MacQueen G, Sherman PM, Perdue MH, 2007 Probiotic treatment of rat pups normalises corticosterone release and ameliorates colonic dysfunction induced by maternal separation. Gut 56, 1522–1528. [PubMed: 17339238]

Grandjean P, Landrigan PJ, 2006 Developmental neurotoxicity of industrial chemicals. Lancet 368, 2167–2178. [PubMed: 17174709]

Herrick RF, Lefkowitz DJ, Weymouth GA, 2007 Soil contamination from PCB-containing buildings. Environ Health Perspect 115, 173–175. [PubMed: 17384760]

Herrick RF, McClean MD, Meeker JD, Baxter LK, Weymouth GA, 2004 An unrecognized source of PCB contamination in schools and other buildings. Environ Health Perspect 112, 1051–1053. [PubMed: 15238275]

Hertz-Picciotto I, Schmidt RJ, Walker CK, Bennett DH, Oliver M, Shedd-Wise KM, LaSalle JM, Giulivi C, Puschner B, Thomas J, Roa DL, Pessah IN, Van de Water J, Tancredi DJ, Ozonoff S, 2018 A Prospective Study of Environmental Exposures and Early Biomarkers in Autism Spectrum Disorder: Design, Protocols, and Preliminary Data from the MARBLES Study. Environ Health Perspect 126, 117004. [PubMed: 30465702]

Hunsaker MR, Greco CM, Spath MA, Smits AP, Navarro CS, Tassone F, Kros JM, Severijnen LA, Berry-Kravis EM, Berman RF, Hagerman PJ, Willemsen R, Hagerman RJ, Hukema RK, 2011 Widespread non-central nervous system organ pathology in fragile X premutation carriers with fragile X-associated tremor/ataxia syndrome and CGG knock-in mice. Acta Neuropathol 122, 467–479. [PubMed: 21785977]

Johansson ME, Jakobsson HE, Holmen-Larsson J, Schutte A, Ermund A, Rodriguez-Pineiro AM, Arike L, Wising C, Svensson F, Backhed F, Hansson GC, 2015 Normalization of Host Intestinal Mucus Layers Requires Long-Term Microbial Colonization. Cell Host Microbe 18, 582–592. [PubMed: 26526499]

Kang DW, Ilhan ZE, Isern NG, Hoyt DW, Howsmon DP, Shaffer M, Lozupone CA, Hahn J, Adams JB, Krajmalnik-Brown R, 2018 Differences in fecal microbial metabolites and microbiota of children with autism spectrum disorders. Anaerobe 49, 121–131. [PubMed: 29274915]

Katoh K, Standley DM, 2013 MAFFT multiple sequence alignment software version 7: improvements in performance and usability. Mol Biol Evol 30, 772–780. [PubMed: 23329690]

Keil KP, Sethi S, Wilson MD, Silverman JL, Pessah IN, Lein PJ, 2019 Genetic mutations in Ca(2+) signaling alter dendrite morphology and social approach in juvenile mice. Genes Brain Behav 18, e12526. [PubMed: 30311737]

Kim S, Kim H, Yim YS, Ha S, Atarashi K, Tan TG, Longman RS, Honda K, Littman DR, Choi GB, Huh JR, 2017 Maternal gut bacteria promote neurodevelopmental abnormalities in mouse offspring. Nature 549, 528–532. [PubMed: 28902840]

Knip M, Siljander H, 2016 The role of the intestinal microbiota in type 1 diabetes mellitus. Nat Rev Endocrinol 12, 154–167. [PubMed: 26729037]

Krueger DD, Bear MF, 2011 Toward fulfilling the promise of molecular medicine in fragile X syndrome. Annu Rev Med 62, 411–429. [PubMed: 21090964]

Kundu P, Blacher E, Elinav E, Pettersson S, 2017 Our Gut Microbiome: The Evolving Inner Self. Cell 171, 1481–1493. [PubMed: 29245010]

Larsen N, Vogensen FK, van den Berg FW, Nielsen DS, Andreasen AS, Pedersen BK, Al Soud WA, Sorensen SJ, Hansen LH, Jakobsen M, 2010 Gut microbiota in human adults with type 2 diabetes differs from non-diabetic adults. PLoS One 5, e9085. [PubMed: 20140211]

Leclercq S, Mian FM, Stanisz AM, Bindels LB, Cambier E, Ben-Amram H, Koren O, Forsythe P, Bienenstock J, 2017 Low-dose penicillin in early life induces long-term changes in murine gut microbiota, brain cytokines and behavior. Nat Commun 8, 15062. [PubMed: 28375200]

Leehey MA, Hagerman PJ, 2012 Fragile X-associated tremor/ataxia syndrome. Handb Clin Neurol 103, 373–386. [PubMed: 21827901]

Lesiak A, Zhu M, Chen H, Appleyard SM, Impey S, Lein PJ, Wayman GA, 2014 The environmental neurotoxicant PCB 95 promotes synaptogenesis via ryanodine receptor-dependent miR132 upregulation. J Neurosci 34, 717–725. [PubMed: 24431430]

Lichtman JS, Alsentzer E, Jaffe M, Sprockett D, Masutani E, Ikwa E, Fragiadakis GK, Clifford D, Huang BE, Sonnenburg JL, Huang KC, Elias JE, 2016 The effect of microbial colonization on the host proteome varies by gastrointestinal location. ISME J 10, 1170–1181. [PubMed: 26574685]

Lozupone C, Lladser ME, Knights D, Stombaugh J, Knight R, 2011 UniFrac: an effective distance metric for microbial community comparison. ISME J 5, 169–172. [PubMed: 20827291]

Lyall K, Croen LA, Sjodin A, Yoshida CK, Zerbo O, Kharrazi M, Windham GC, 2017 Polychlorinated Biphenyl and Organochlorine Pesticide Concentrations in Maternal MidPregnancy Serum

Samples: Association with Autism Spectrum Disorder and Intellectual Disability. Environ Health Perspect 125, 474–480. [PubMed: 27548254]

Mayer EA, Knight R, Mazmanian SK, Cryan JF, Tillisch K, 2014 Gut microbes and the brain: paradigm shift in neuroscience. J Neurosci 34, 15490–15496. [PubMed: 25392516]

Mitchell MM, Woods R, Chi LH, Schmidt RJ, Pessah IN, Kostyniak PJ, LaSalle JM, 2012 Levels of select PCB and PBDE congeners in human postmortem brain reveal possible environmental involvement in 15q11-q13 duplication autism spectrum disorder. Environ Mol Mutagen 53, 589–598. [PubMed: 22930557]

Mukherjee T, Hovingh ES, Foerster EG, Abdel-Nour M, Philpott DJ, Girardin SE, 2018 NOD1 and NOD2 in inflammation, immunity and disease. Arch Biochem Biophys.

Norstrom K, Czub G, McLachlan MS, Hu D, Thorne PS, Hornbuckle KC, 2010 External exposure and bioaccumulation of PCBs in humans living in a contaminated urban environment. Environ Int 36, 855–861. [PubMed: 19394084]

Owino V, Ahmed T, Freemark M, Kelly P, Loy A, Manary M, Loechl C, 2016 Environmental Enteric Dysfunction and Growth Failure/Stunting in Global Child Health. Pediatrics 138.

Paliy O, Shankar V, 2016 Application of multivariate statistical techniques in microbial ecology. Mol Ecol 25, 1032–1057. [PubMed: 26786791]

Pessah IN, Cherednichenko G, Lein PJ, 2010 Minding the calcium store: Ryanodine receptor activation as a convergent mechanism of PCB toxicity. Pharmacol Ther 125, 260–285. [PubMed: 19931307]

Petriello MC, Hoffman JB, Vsevolozhskaya O, Morris AJ, Hennig B, 2018 Dioxin-like PCB 126 increases intestinal inflammation and disrupts gut microbiota and metabolic homeostasis. Environ Pollut 242, 1022–1032. [PubMed: 30373033]

Price MN, Dehal PS, Arkin AP, 2010 FastTree 2--approximately maximum-likelihood trees for large alignments. PLoS One 5, e9490. [PubMed: 20224823]

Pusceddu MM, El Aidy S, Crispie F, O'Sullivan O, Cotter P, Stanton C, Kelly P, Cryan JF, Dinan TG, 2015 N-3 Polyunsaturated Fatty Acids (PUFAs) Reverse the Impact of Early-Life Stress on the Gut Microbiota. PLoS One 10, e0139721. [PubMed: 26426902]

Pusceddu MM, Murray K, Gareau MG, 2018 Targeting the Microbiota, from Irritable Bowel Syndrome to Mood Disorders: Focus on Probiotics and Prebiotics. Curr Pathobiol Rep 6, 1–13. [PubMed: 29785336]

Quast C, Pruesse E, Yilmaz P, Gerken J, Schweer T, Yarza P, Peplies J, Glockner FO, 2013 The SILVA ribosomal RNA gene database project: improved data processing and web-based tools. Nucleic Acids Res 41, D590–596. [PubMed: 23193283]

Reardon C, Lechmann M, Brustle A, Gareau MG, Shuman N, Philpott D, Ziegler SF, Mak TW, 2011 Thymic stromal lymphopoetin-induced expression of the endogenous inhibitory enzyme SLPI mediates recovery from colonic inflammation. Immunity 35, 223–235. [PubMed: 21820333]

Rizzatti G, Lopetuso LR, Gibiino G, Binda C, Gasbarrini A, 2017 Proteobacteria: A Common Factor in Human Diseases. Biomed Res Int 2017, 9351507. [PubMed: 29230419]

Robin G, Lopez JR, Espinal GM, Hulsizer S, Hagerman PJ, Pessah IN, 2017 Calcium dysregulation and Cdk5-ATM pathway involved in a mouse model of fragile X-associated tremor/ataxia syndrome. Hum Mol Genet 26, 2649–2666. [PubMed: 28444183]

Robson M, Melymuk L, Csiszar SA, Giang A, Diamond ML, Helm PA, 2010 Continuing sources of PCBs: the significance of building sealants. Environ Int 36, 506–513. [PubMed: 20452025]

Rose DR, Yang H, Serena G, Sturgeon C, Ma B, Careaga M, Hughes HK, Angkustsiri K, Rose M, Hertz-Picciotto I, Van de Water J, Hansen RL, Ravel J, Fasano A, Ashwood P, 2018 Differential immune responses and microbiota profiles in children with autism spectrum disorders and co-morbid gastrointestinal symptoms. Brain Behav Immun 70, 354–368. [PubMed: 29571898]

Sagiv SK, Thurston SW, Bellinger DC, Altshul LM, Korrick SA, 2012 Neuropsychological measures of attention and impulse control among 8-year-old children exposed prenatally to organochlorines. Environ Health Perspect 120, 904–909. [PubMed: 22357172]

Sagiv SK, Thurston SW, Bellinger DC, Tolbert PE, Altshul LM, Korrick SA, 2010 Prenatal organochlorine exposure and behaviors associated with attention deficit hyperactivity disorder in school-aged children. Am J Epidemiol 171, 593–601. [PubMed: 20106937]

Sanctuary MR, Kain JN, Angkustsiri K, German JB, 2018 Dietary Considerations in Autism Spectrum Disorders: The Potential Role of Protein Digestion and Microbial Putrefaction in the Gut-Brain Axis. Front Nutr 5, 40. [PubMed: 29868601]

Schantz SL, Widholm JJ, Rice DC, 2003 Effects of PCB exposure on neuropsychological function in children. Environ Health Perspect 111, 357–576. [PubMed: 12611666]

Sethi S, Morgan RK, Feng W, Lin Y, Li X, Luna C, Koch M, Bansal R, Duffel MW, Puschner B, Zoeller RT, Lehmler HJ, Pessah IN, Lein PJ, 2019 Comparative Analyses of the 12 Most Abundant PCB Congeners Detected in Human Maternal Serum for Activity at the Thyroid Hormone Receptor and Ryanodine Receptor. Environ Sci Technol.

Sharkey KA, Beck PL, McKay DM, 2018 Neuroimmunophysiology of the gut: advances and emerging concepts focusing on the epithelium. Nat Rev Gastroenterol Hepatol 15, 765–784. [PubMed: 30069036]

Stamou M, Streifel KM, Goines PE, Lein PJ, 2013 Neuronal connectivity as a convergent target of gene x environment interactions that confer risk for Autism Spectrum Disorders. Neurotoxicol Teratol 36, 3–16. [PubMed: 23269408]

Wayman GA, Yang D, Bose DD, Lesiak A, Ledoux V, Bruun D, Pessah IN, Lein PJ, 2012 PCB-95 promotes dendritic growth via ryanodine receptor-dependent mechanisms. Environ Health Perspect 120, 997–1002. [PubMed: 22534141]

Willemsen R, Hoogeveen-Westerveld M, Reis S, Holstege J, Severijnen LA, Nieuwenhuizen IM, Schrier M, van Unen L, Tassone F, Hoogeveen AT, Hagerman PJ, Mientjes EJ, Oostra BA, 2003 The FMR1 CGG repeat mouse displays ubiquitin-positive intranuclear neuronal inclusions; implications for the cerebellar tremor/ataxia syndrome. Hum Mol Genet 12, 949–959. [PubMed: 12700164]

Yang D, Kim KH, Phimister A, Bachstetter AD, Ward TR, Stackman RW, Mervis RF, Wisniewski AB, Klein SL, Kodavanti PR, Anderson KA, Wayman G, Pessah IN, Lein PJ, 2009 Developmental exposure to polychlorinated biphenyls interferes with experience-dependent dendritic plasticity and ryanodine receptor expression in weanling rats. Environ Health Perspect 117, 426–435. [PubMed: 19337518]

Zhu MH, Sung TS, O'Driscoll K, Koh SD, Sanders KM, 2015 Intracellular Ca(2+) release from endoplasmic reticulum regulates slow wave currents and pacemaker activity of interstitial cells of Cajal. Am J Physiol Cell Physiol 308, C608–620. [PubMed: 25631870]

HIGHLIGHTS

1. Developmental PCBs cause intestinal pathophysiology, inflammation, and dysbiosis of the microbiota in juvenile mice harboring mutations affecting normal Ca^{2+} signaling.
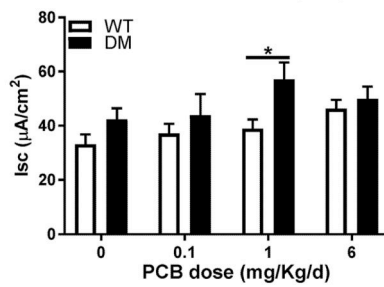
2. Intestinal pathophysiology is accompanied by changes in tissue cytokine expression in both the ileum and colon in a tissue specific, dose specific, and genotype specific manner.

3. Developmental PCBs in a genetically susceptible host causes intestinal dysbiosis in juvenile mice characterized by altered diversity and colonization of specific taxa.

Developmental PCBs cause intestinal pathophysiology, inflammation, and dysbiosis of the microbiota in juvenile mice harboring mutations impairing Ca^{2+} signaling.
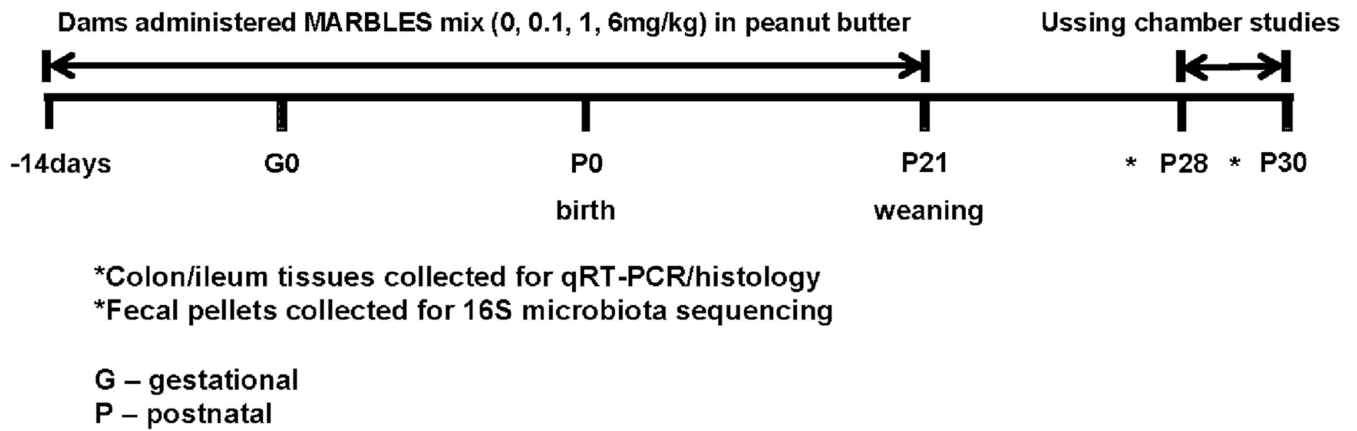
Figure 1. Study time course.

Exposure to PCBs commenced in mouse dams starting two weeks prior to gestation and continued until weaning of the pups at postnatal day (P)21. Intestinal samples for Ussing chamber studies and tissues (colon, ileum, feces) were collected at P28-P30.
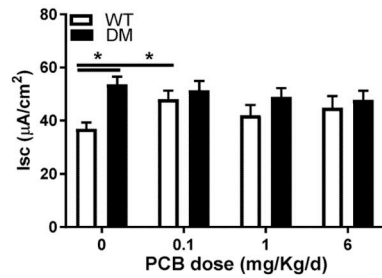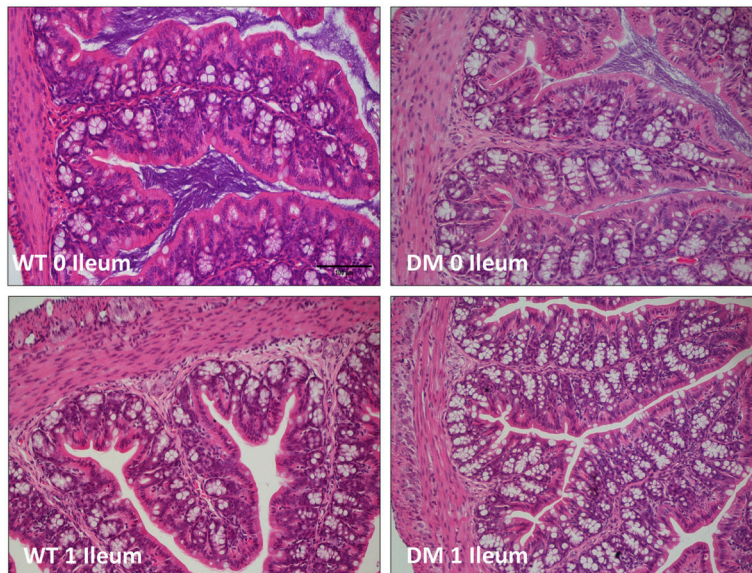
Colon

Figure 2. Colonic physiology is impaired following developmental PCB exposure in juvenile DM mice.

(**A**) Secretory state (short-circuit current (Isc); and (**B, C**) permeability (conductance (G); FITC dextran flux) were measured in the colon in both WT and DM juvenile mice developmentally exposed to PCBs (0, 0.1, 1,6 mg/kg/d); the right FITC panel represents the 1mg/kg/d dose in WT (left) and DM (middle) panels for direct comparison. (N = 10-15 per group) (**D**) Representative histological images (H&E stained; 20X magnification; N = 4

taken per group). Data are presented as mean ± SEM; *P < 0.05; **P < 0.01, 2-way ANOVA.

Ileum

A. Short circuit current (Isc)

B. Conductance (G)
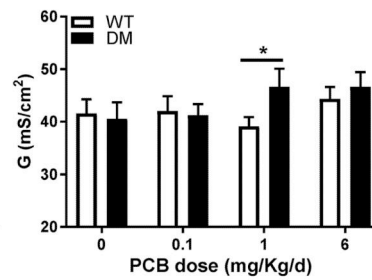
C. FITC flux
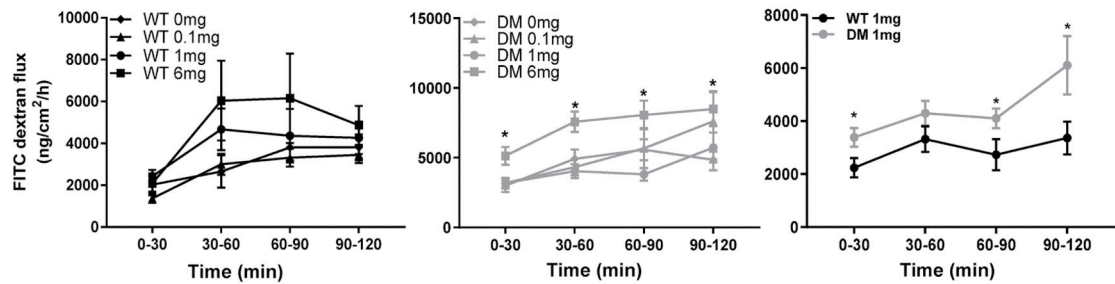
D. Histology

Figure 3. Ileal physiology is impaired following developmental PCB exposure in juvenile DM mice.
(**A**) Secretory state (short-circuit current (Isc); and (**B, C**) permeability (conductance (G); FITC dextran flux) were measured in the ileum in both WT and DM mice developmentally exposed to PCBs (0, 0.1, 1,6 mg/kg/d); the right FITC panel represents the 1 mg/kg/d dose in WT (left) and DM (middle) panels for direct comparison. (**D**) Representative histological images (H&E stained; 20X magnification). Data are presented as mean ± SEM; N = 10-15 per group. *P < 0.05; **P < 0.01, 2-way ANOVA.
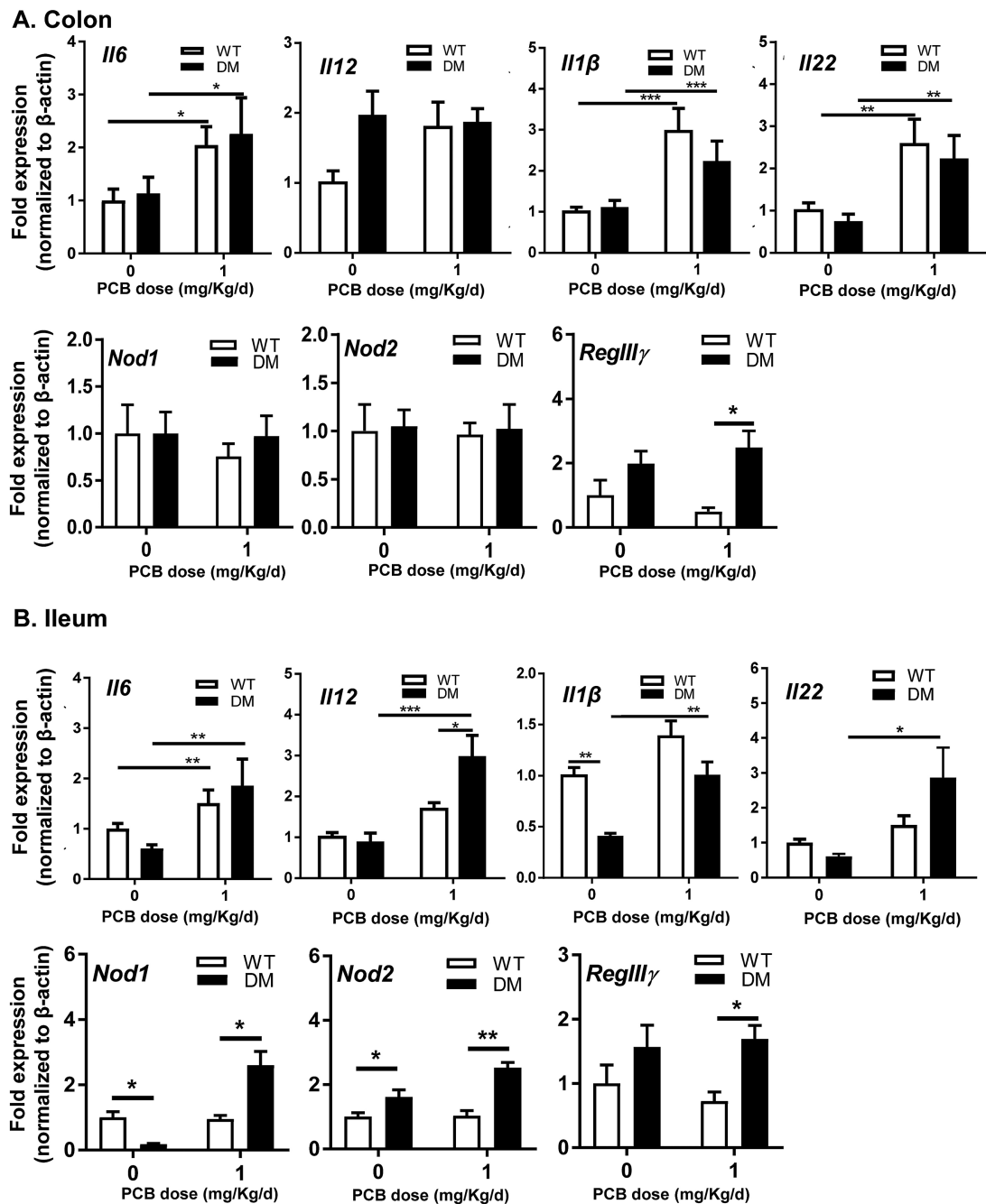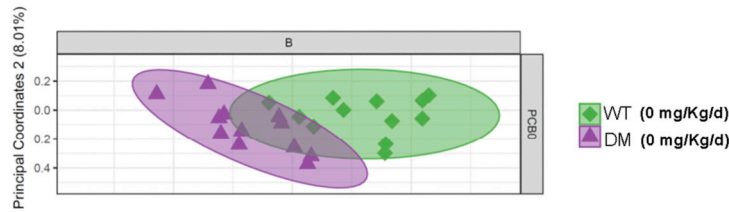
A. Colon

B. Ileum

Figure 4. Expression of immune markers and cytokines is altered in the GI tract following PCB exposure.

Samples from the (**A**) colon and (**B**) ileum were analyzed by qPCR for *Il6, Il12, Il1β, Il22, Nod1, Nod2* and *RegIIIγ*. Data are presented as mean ± SEM; N = 6-8 per group. *P < 0.05, 2-way ANOVA.
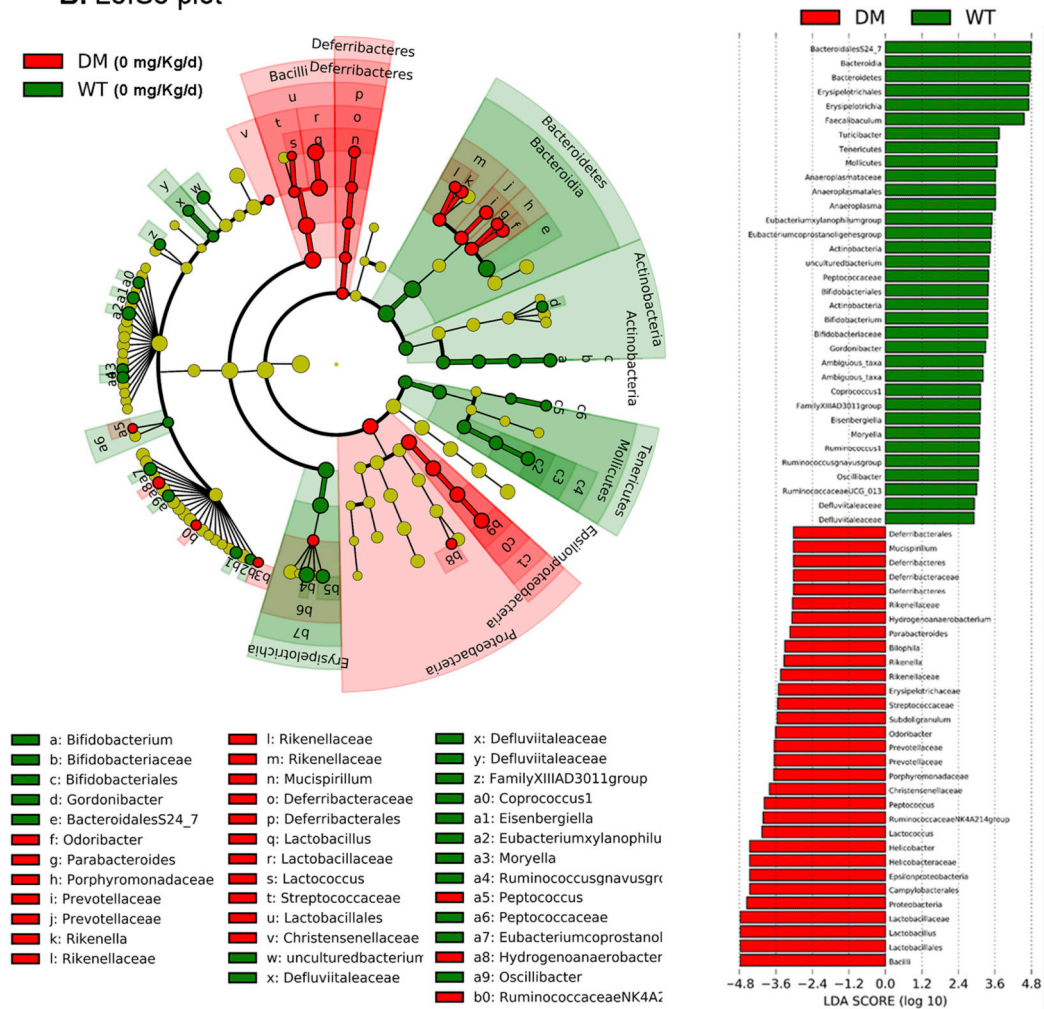
Figure 5. Differences in the gut microbiota are observed in beta diversity in DM mice following PCB exposure.

(**A**) Analysis for β-diversity was processed using the Bray-Curtis method with each panel representing both WT vs DM mice at 0 and 1 mg/kg/d PCB exposure. (**B**) Linear discriminant analysis effect size (LEfSe) was used to identify the most differentially abundant taxa between vehicle-treated WT and DM mice as represented by a cladogram (inner to outer rings: phylum, class, order, family, and genus), and their effect size (linear discriminate analysis [LDA] score plot). N = 11 mice per group.
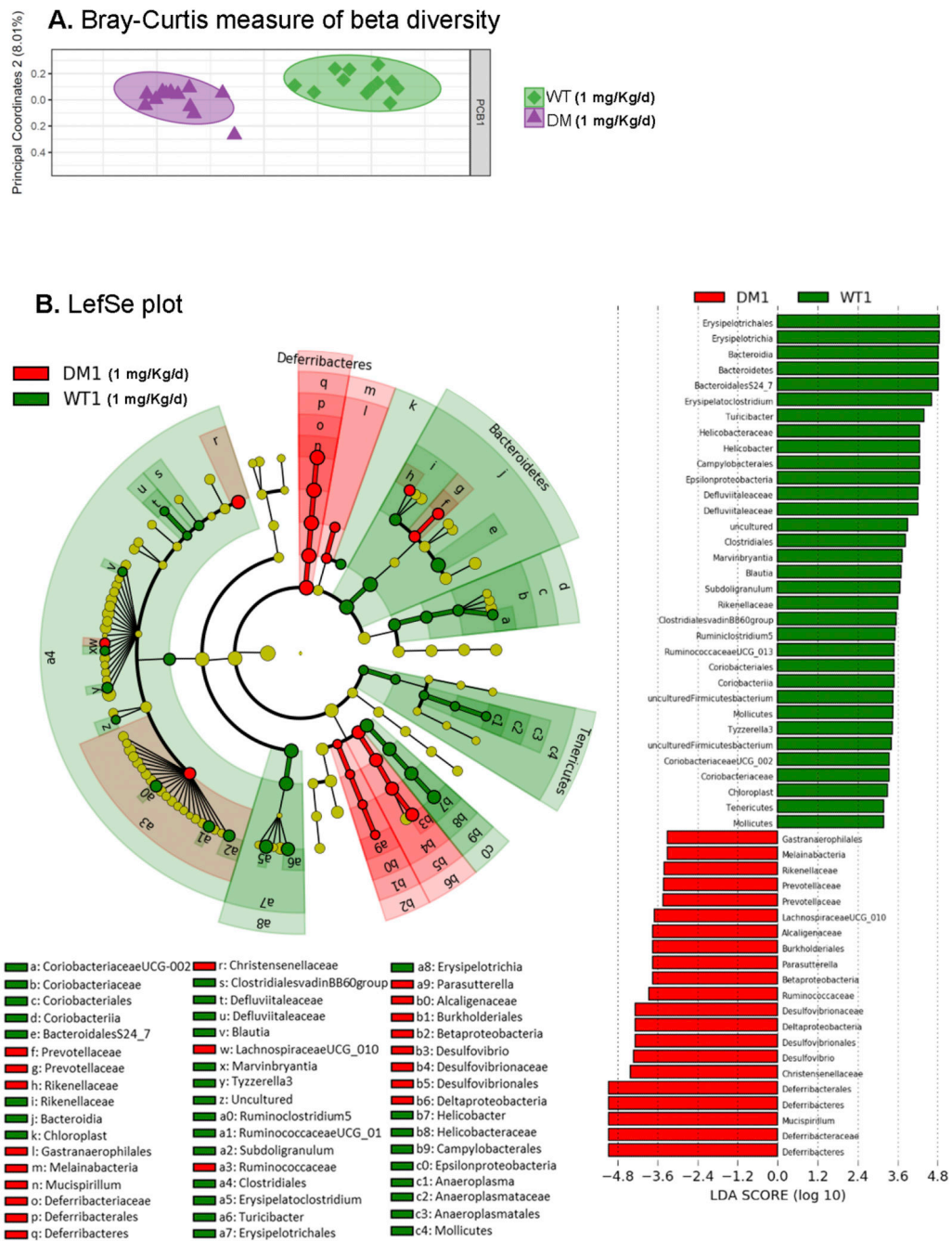
Figure 6. Differences in the gut microbiota are observed in beta diversity in DM mice following PCB exposure.

Linear discriminant analysis effect size (LEfSe) was used to identify the most differentially abundant taxa between WT and DM mice exposed developmentally to PCBs at 1 mg/kg/d, as represented by a cladogram (inner to outer rings: phylum, class, order, family, and genus), and their effect size (linear discriminate analysis [LDA] score plot). N = 11 mice per group.
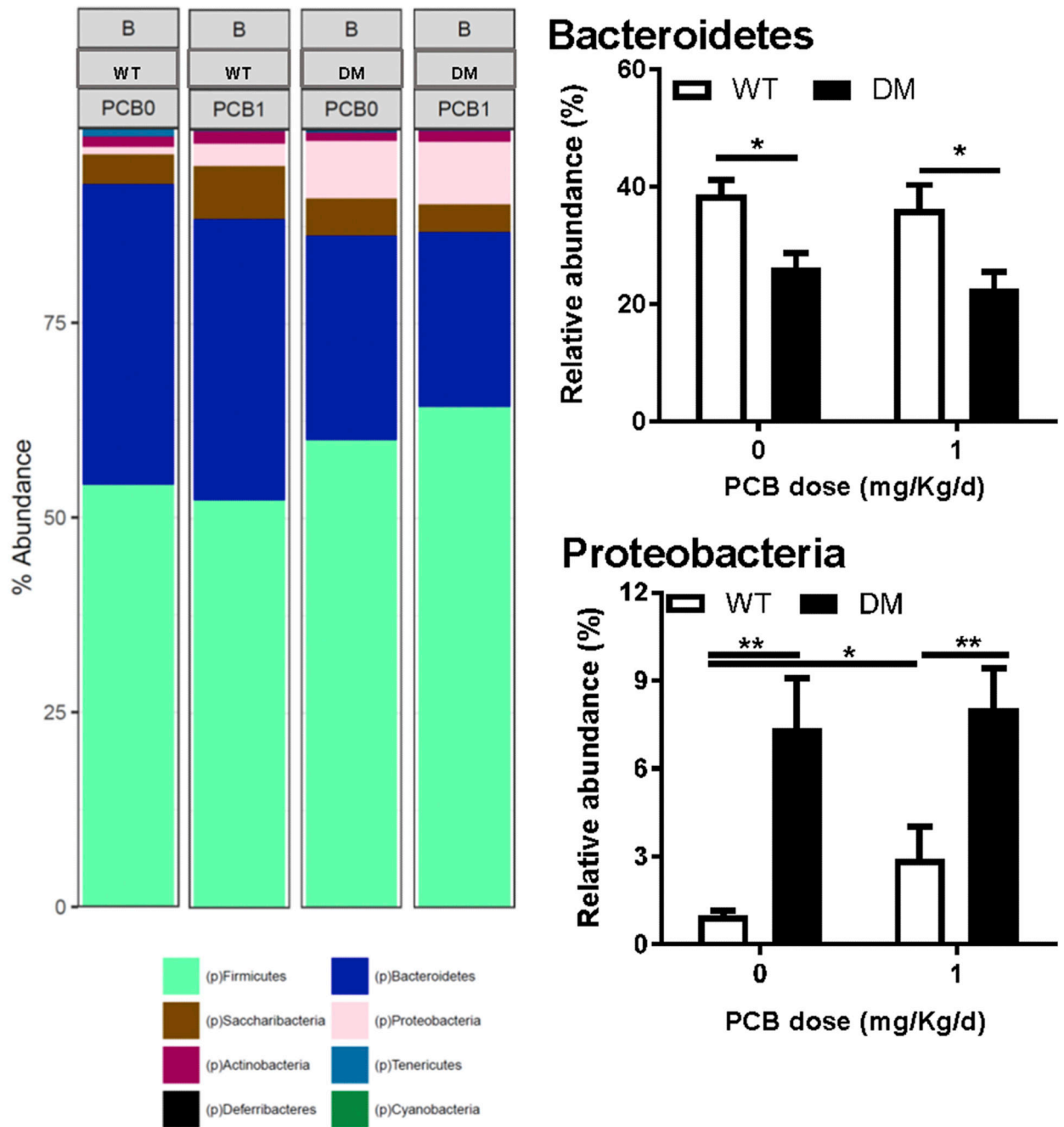
Figure 7. Differences in microbiota abundance are observed at the phylum level in DM mice following PCB exposure.

Representation of the relative abundance at the phylum level in WT vs DM mice exposed to vehicle (0 mg/kg/d) or PCBs (1 mg/kg/d). Data are presented as mean ± SEM; N = 6 mice per group. *P < 0.05; **p<0.01, 2-way ANOVA.
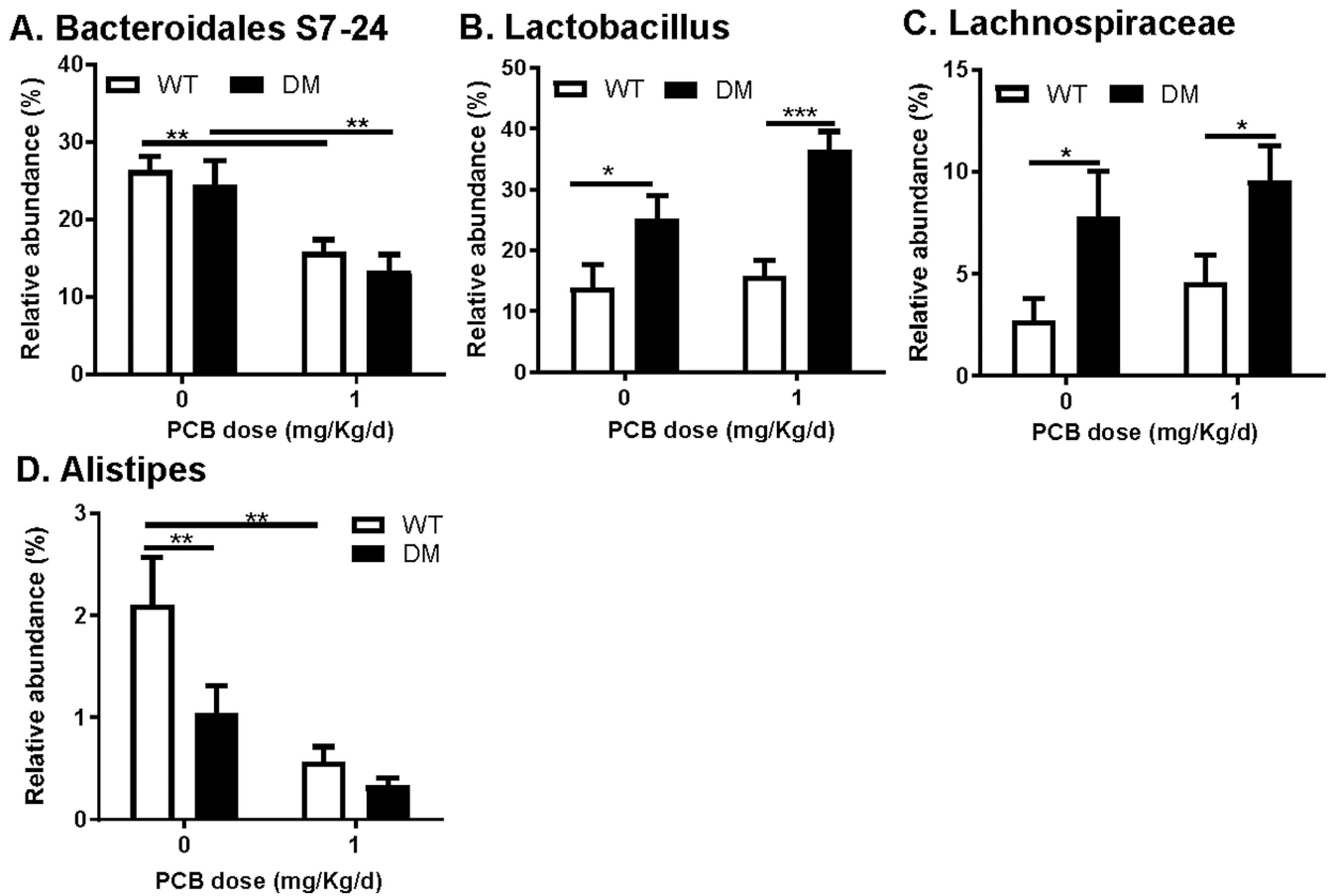
Figure 8. Changes in microbiota are observed in genus abundance following PCB exposure in DM mice.

Representation of the relative abundance (%) at the genus level of Bacteroidales S7-24, Lactobacillus, Lachnospiraceae and Alistipes between WT and DM mice following 0 or 1 mg/kg PCB exposure. Data are presented as mean ± SEM; N = 6 mice per group. *P < 0.05; **P < 0.01; ***P < 0.001,2-way ANOVA.

Table 1.

Primer sequences

Gene	Forward (5′ - 3′)	Reverse (5′ - 3′)
Nod2	CACACATGGCCTTTGGTTCCAGT	AAAGAGCTGCAGTTGAGGGAGGAA
Nod1	TCCCTTGCCTGTGAGCAGAAAGTA	GTGGGTATGTGCCATGCTTTGCTT
β-actin	GGCTGTATTCCCCTCCATCG	CCAGTTGGTAACAATGCCATGT
RegIIIγ	TTCCTGTCCTCCATGATCAAAA	CATCCACCTCTGTTGGGTTCA
Il12	TGGTTTGCCATCGTTTTGCTG	ACAGGTGAGGTTCACTGTTTCT
Il22	ATGAGTTTTTCCCTTATGGGGAC	GCTGGAAGTTGGACACCTCAA
Il6	TAGTCCTTCCTACCCCAATTTCC	TTGGTCCTTAGCCACTCCTTC
Il1β	CTGTGACTCATGGGATGATGATG	CGGAGCCTGTAGTGCAGTTG

TABLE 2 –

Statistical analysis for Bray-Curtis plot

PERMANOVA						
Group 1	**Group 2**	**Sample Size**	**Permutations**	**pseudo-F**	**p-value**	**q-value**
DM	WT	24	999	5.171308	0.001	0.001556
DM1	WT1	24	999	12.53999	0.001	0.001556
ANOSIM						
Group 1	**Group2**	**Sample Size**	**Permutations**	**R**	**p-value**	**q-value**
DM	WT	24	999	0.501368	0.001	0.001474
DM1	WT1	24	999	0.925926	0.001	0.001474
PERMDISP						
Group 1	**Group 2**	**Sample size**	**Permutations**	**F-value**	**p-value**	**q-value**
DM	WT	24	999	0.524636	0.465	0.765882
DM1	WT1	24	999	5.647727	0.002	0.014